Published in final edited form as:
*Int J Radiat Oncol Biol Phys*. 2011 January 1; 79(1): 269–278. doi:10.1016/j.ijrobp.2010.02.052.

# Real-time target position estimation using stereoscopic kV/MV imaging and external respiratory monitoring for dynamic MLC tracking

**Byungchul Cho, PhD**[1], **Per Rugaard Poulsen, PhD**[1,2], **Amit Sawant, PhD**[1], **Dan Ruan**[1], and **Paul J Keall, PhD**[1]

[1] Department of Radiation Oncology, Stanford University, Stanford, CA

[2] Department of Medical Physics, Department of Radiation Oncology, Aarhus University, Denmark

## Abstract

**Purpose—**To develop a real-time target position estimation method using stereoscopic kV/MV imaging and external respiratory monitoring, and investigate the performance of a dynamic MLC tracking system employing this method.

**Method and Materials—**Real-time 3D internal target position estimation was established by creating a time-varying correlation model that connects external respiratory signals with internal target motion measured intermittently by kV/MV imaging. The method was integrated into a dynamic MLC tracking system. Tracking experiments were performed for 10 thoracic/abdominal traces. A 3D motion platform carrying a gold marker and a separate 1D motion platform were used to reproduce the target and external respiratory motion, respectively. Target positions were detected by kV (1Hz) and MV (5.2Hz) imaging, while external respiratory motion was captured by an optical system (30Hz). Beam-target alignment error was quantified as the positional difference between the target and circular beam-center on MV images acquired during tracking. Correlation model error was quantified by comparing a model estimate and measured target positions.

**Results—**The root-mean-square errors (RMSE) in beam-target alignment that ranged from 3.1 to 7.6mm without tracking were reduced to less than 1.5 mm with tracking, except during the model-building period (6 sec). The RMSE in the correlation model was sub-mm in all directions.

**Conclusions—**A novel real-time target position estimation method has been developed and integrated into a dynamic MLC tracking system demonstrating on average sub-mm geometric accuracy after initializing the internal/external model. The method uses hardware tools available on linear accelerators and therefore shows promise for clinical implementation.

Corresponding Author: Byungchul Cho, PhD, Department of Radiation Oncology, Asan Medical Center, 86 Asanbyeonwon-gil, Songpa-gu, Seoul, 138-736, Korea.

**Conflict of Interest Notification:** Research supported by NIH/NCI R01-93626.
Per Rugaard Poulsen has received financial support from Varian Medical Systems.

### Keywords

Real-time tumor tracking; X-ray image guidance; External respiratory surrogate; respiratory tumor motion; Dynamic multileaf collimator

## Introduction

Many linear accelerators have both gantry-mounted kilovoltage (kV) and megavoltage (MV) imaging systems, which are actively being used for tumor localization and volumetric imaging, but are not routinely used for tumor tracking. In an effort to utilize the imaging systems for intrafraction motion management of thoracic and abdominal tumors, we have recently developed a direct real-time target position monitoring method using a gantry-mounted kV/MV imaging system (1,2) and a gantry mounted kV imaging system (3). These methods demonstrate experimental accuracy of sub-2mm, however both methods require continuous kV imaging that gives additional unwanted dose to the patient. Additionally, the large system latency of 450 ms (1) and 570 ms (3) caused by handling large-sized digital kV/MV images reduced the tracking accuracy. One feasible approach to reduce x-ray imaging dose and latency would be a hybrid position monitoring strategy (4), where direct stereoscopic x-ray measurement of internal target position is supplemented with external respiratory signals. The respiratory motion is continuously monitored by external surrogates and correlated with the tumor motion that is measured via kV/MV imaging. CyberKnife (Accuray, Sunnyvale, CA) implements a target tracking scheme by continuously monitoring an external surrogate of the respiratory motion and correlates it with the internal tumor motion measured by kV/kV imaging (4). Unfortunately, wide use of this tracking system is limited by the radiosurgery specifications of the CyberKnife. Following a similar rationale we have developed a hybrid method utilizing gantry-mounted kV/MV imaging and external respiratory monitoring systems that are readily available with conventional treatment machines. With a dynamic multileaf collimator (DMLC) tracking system employing this method, tracking performance was investigated through experiments.

## Method and Materials

### Real-time target position estimation with dynamic MLC tracking

An external respiratory surrogate, a Real-time Position Management (RPM) System (Varian Medical Systems, Palo Alto, CA), was incorporated into a previously described experimental system (1), where target position was measured directly using gantry-mounted kV/MV imaging systems. In the current study, the kV/MV image information is augmented by the external signal and an internal/external correlation model established to estimate real-time target position. The target position estimate is fed into a DMLC tracking system to continuously align the beam with the moving target. The integrated DMLC tracking system and the procedure of real-time target position estimation are illustrated in Fig. 1.

The procedure of a real-time target position estimation using occasional kV/MV imaging and continuous external respiratory monitoring is as follows (the step numbers refer to Fig. 1).

- Step 1-3: as described in detail in the previous work (1), the internal target motion reproduced by a gold marker-embedded phantom on a 3D motion platform (5) is captured by the kV and MV imaging systems. Immediately after the acquired image has been stored on each workstation, a segmentation program extracts the gold-marker position from the image and sends it to the DMLC tracking program.

- Step 4: once the tracking program receives a kV (or MV) gold-marker position, it finds the synchronized RPM data based on the measured offset (see *synchronization* below). The 3D target position is calculated with each kV image by triangulation with the MV images. For each kV image, the MV images acquired immediately before and after it are first used for independent triangulation -- these two intermediate triangulation results are then interpolated to minimize the synchronization mismatch between the kV/MV pair.
- Step 5: Meanwhile, an RPM block is placed on a separate 1D motion platform, which reproduces external respiratory motion data synchronized with the internal 3D tumor motion. The block is monitored by the RPM system, which feeds the optical information to the DMLC tracking program at 30Hz.
- Step 6: The 3D target position from step 4 and the synchronized RPM data from step 5 are used to update the correlation model. When new RPM data arrives, prediction is first applied to compensate for the system latency, and then the 3D target position is inferred from the predicted RPM data through the correlation model.
- Step 7-8: Finally, MLC leaf positions are calculated from the estimated 3D target position and sent to the DMLC controller. The DMLC controller repositions the MLC leaves to match the updated 3D target position (6).

### Synchronization of kV/MV and RPM data streams

The internal target positions from kV/MV images and external signals from the RPM system experience different time delays between the moment of acquisition and their arrival at the DMLC tracking computer. Addressing this time discrepancy and accurately synchronizing these elements is essential to build an accurate correlation model. For this purpose, the following experiment was performed. While 3D phantom motion of a 2cm peak-to-peak sinusoidal SI motion with 20-sec period was captured by the kV/MV imaging, synchronous 1D motion of a 2cm peak-to-peak sinusoidal AP motion was monitored by the RPM system. By recording the arrival time on the tracking computer for the kV, MV, and RPM data streams using a known input, the relative time offsets for synchronization was measured, i.e., the gold seed positions from the kV (or MV) images and the RPM signals as a function of the arrival time were fit to sinusoidal curves and the time delay of the kV (or MV) image data were calculated from the phase shift of the kV (or MV) fit curve with respect to the RPM curve.

In the present study we reduced the kV imaging frequency down to 1Hz in order to demonstrate the reduction of the kV imaging dose to the patient. On the other hand, since MV imaging uses the treatment beam without additional imaging dose cost, it could be utilized to full capacity. MV imaging frequency of 5.2Hz at 200 MU/min was chosen to obtain kV image quality appropriate for marker segmentation while fluoroscopic kV images were acquired at 1Hz. One noticeable issue with the OBI imaging system is that an acquired fluoroscopic image is not stored until the next image in the series has been taken. Consequently, time delay from acquisition to triangulation is always larger than the kV imaging interval. The kV images acquired at 1Hz are only available for triangulation after 1 sec plus additional time required for image processing and marker extraction. The arrival times of the kV and MV data were 1088 ± 37 ms and 263 ± 28 ms delayed, respectively, compared to the RPM signal. Each kV (or MV) image is synchronized with the RPM data based on this measurement for the correlation model.

Note that even though the large delay of kV data due to the low imaging frequency delayed calculating the target position, it is not critical for real-time tracking because the measured

target position is only used for the correlation model, while the estimation of the target position itself is updated promptly from the external signal. Hence, the overall latency of the integrated tracking system is only affected by the delay of RPM data.

## Correlation model

For the correlation model (Step 6) we adapted a state-augmented linear method (7) which can implicitly resolve the potential hysteresis between the internal target motion and the external signal. Each motion component of the 3D target position $\mathbf{T}(t)$ is continuously estimated by the external respiratory signal $R(t)$ through the correlation model;

$$\begin{pmatrix} T_x \\ T_y \\ T_z \end{pmatrix} = \begin{pmatrix} a_x \\ a_y \\ a_z \end{pmatrix} R(t) + \begin{pmatrix} b_x \\ b_y \\ b_z \end{pmatrix} R(t-\tau) + \begin{pmatrix} c_x \\ c_y \\ c_z \end{pmatrix}.$$

The lag time interval $\tau$ needs to be short enough to reflect local dynamics but also long enough to minimize the effect of noise. $\tau = 0.5$ sec was chosen though the results of the current study were found to be insensitive to this parameter value. The model parameters (**a,b,c**) can be determined by intermittently acquired target positions $\mathbf{T}(t_i)$ using kV/MV imaging and synchronous external signal $R(t_i)$ by least-squares estimation, i.e., minimizing the estimation error for each component of the internal target motion;

$$\sum_{i=1}^{N} ||T_x(t_i) - (a_x R(t_i) + b_x R(t-\tau) + c_x||^2,$$

and similarly for y and z. Here, $N$ is the number of synchronized measurements of $\mathbf{T}(t_i)$ and $R(t_i)$ used in the model. The correlation model was first established with $N = 5$ using the five 3D target positions measured by the same number of kV images acquired. After that, each time a new target position was measured with kV imaging, the model was updated with the latest 15 (if available) target positions.

## System latency and prediction

The latency of the entire tracking system was measured by the method described in the previous study (1). The measured delay time was 160 ms, which was the same result as with the previous RPM-alone based tracking (8). This value was applied for a linear adaptive filter-based prediction (9) to compensate for the overall system latency.

## Tracking experiments

Ten tumor trajectories and associated external respiratory signals with a motion range larger than 10 mm were selected from 160 tumor trajectories (10) acquired from 46 thoracic/abdominal tumor patients treated by a CyberKnife Synchrony system. The beginning 110-sec part of each trajectory was used for the tracking experiment that was composed of the prediction training (40 sec) and tracking (60 sec) periods. The mean (range) of the peak-to-peak motion of the selected trajectories was 6.4 (1.2 - 20.8) mm, 13.0 (1.0 - 20.4) mm, and 5.7 (1.8 - 13.7) mm in the left-right (LR), superior-interior (SI), and anterior-posterior (AP) directions, respectively. The mean (range) of their average breathing cycles was 3.8 (2.7 - 4.9) sec.

Although this method can be used for both static- or rotating-gantry treatment, the entire experiment was performed at a fixed gantry angle such that the MV beam went down vertically and the kV imager was located at the left side of a patient in supine head-first position.

The experiment starts with the 40-s external respiratory data acquisition for prediction training. The experiment starts with a 40-s prediction training phase, during which only external respiratory data (in our case RPM signal) is acquired. After the prediction is enabled, kV/MV imaging starts with MV beam on. Since the correlation model is initialized with five 3D target position measurements, the actual reposition of the MLC leaves begins 6 sec after the MV beam starts. DMLC tracking with 6 MV and a circular MLC aperture of 10-cm diameter continued for one minute, until delivering 200 MU at the dose rate of 200 MU/min. With this dose rate, the MV imaging was acquired with 0.69 MU per image at the rate of 5.2Hz (or equivalently 192 ms imaging interval). For each trajectory the collimator angle was set such that the MLC leaf travel direction matched the major motion direction in either the SI or LR direction.

To investigate the tracking performance, the following data analyses were given for each tracking experiment.

1. The *beam-target alignment error*, i.e., the beam alignment accuracy to the target position on beam's eye view, was quantified as the distance between the marker position and the center of a circular MLC aperture in each direction on all MV images.
2. For each time the correlation model was updated by a new triangulated target position, the estimated target position using the updated model was recorded. The *correlation model error* was quantified by the difference between the triangulated and estimated target position for each motion component.
3. The actual external respiratory input and the predicted data were recorded during the tracking experiments. The *prediction error* was quantified as the difference between the predicted external position and the corresponding actual input that was acquired 160ms later to account for the system latency.
4. Each time external data arrived, the prediction was applied and the target position was estimated via the correlation model with the predicted external data and the lag external data. The estimated 3D target positions were recorded and compared with platform trajectory input. The *target position estimation error* was quantified by the discrepancy between the estimated and the platform input target positions. Note that while the correlation model error does not include the error contribution from prediction, the target position estimation error is the combination of the correlation model and prediction error.

## Results

Fig. 2 shows examples of the beam-target alignment errors measured as the positional differences between the target and beam center on MV images. Regardless of fast breathing motion, irregularities in amplitude or baseline drift, the DMLC tracking with the proposed target positioning method compensates such target motions effectively. As shown by the histograms in Fig. 2, the errors without tracking distribute broadly over the motion range and tend to have peaks at the end of the range, which can be expected from the probability density function of respiratory motion. These error distributions become narrower and close to Gaussian distribution with tracking. The trajectory of the beam shows that the MLC aperture began to follow the target motion ~6 sec after the MV beam started, and caused a large tracking error. During this period five kV images were acquired at 1-sec intervals and then used for the initialization of the correlation model. Note that a systematic shift between the target and beam positions in the lateral direction is still within the machine accuracy of the MV beam isocenter (0.5 mm) stated by the manufacturer. It could be further improved

via calibrating and correcting the MV beam isocenter based on gantry and collimator rotation.

Right after tracking started, beam hold was often asserted by the MLC controller when the difference between the set leaf-position by the DMLC tracking system and the actual leaf-position was beyond the tolerance, which was 5 mm in the experiment. The tracking was resumed ~3 sec later when the MLC caught up with the target motion.

Fig. 3 shows a typical example of the correlation model error and the prediction error. The correlation model error is sub-millimeter in all directions and caused by the inherently incomplete linear correlation between the target motion and external signal. Other external sources of error contributions would be the external signal noise and the imperfect synchronization between external signal, kV, and MV data.

It is important to note that Synchrony tumor trajectory data was not measured directly from the dual kV imaging system, but driven by an external signal through a correlation model similar to the method used in this study (4). Consequently, the tumor trajectory used in this study is likely to better correlate with the external signal compared to the expectation from the real situation, and therefore the correlation model error should be underestimated. We previously addressed this issue and assessed the variation of the model-driven estimated position from the measured target position using Synchrony log files (11). The population mean of root-mean-squared error (RMSE) distributions in 3D was 1.5 ± 0.8 mm, which could be converted to 0.8 mm in each direction assuming the error distributed evenly in all directions. This result agreed with a recent study (12) that used the same methodology and found that the mean correlation model error was 0.4 mm, 0.8 mm, and 0.8 mm for the LR, SI, and AP directions. This suggests that the actual correlation model error would be increased to this amount.

For the ten experiments, prediction reduces more than 50% of the error that might be caused by the system latency without prediction. The prediction performance shows that it is not sensitive to the motion range of the external signal, or irregularities in amplitude, phase, and baseline.

Fig. 4 shows the target position estimation error that was caused by the both contributions from the correlation model and prediction errors shown in Fig. 3. The estimated positions were used to reposition the MLC leaf positions.

Fig. 5 shows overall tracking accuracy for the 10 experimental trajectories. Tracking reduces the beam-target alignment error substantially compared to no-tracking. The beam-target alignment error of no-tracking is likely to be proportional to the range of the motion; in contrast, the beam-target alignment error of tracking is not. The RMSE in the beam-target alignment error including the model building time period was <2.5 mm for one minute tracking. As the tracking time increases these values would converge to <1.5 mm that correspond to the error excluding the model building interval. The error contributions from the correlation model and the prediction are also presented in Fig. 5 for comparison. The RMSE of the prediction error (1D) was below 0.5 mm and the RMSE of the correlation model error (2D) matched with the beam-target alignment error, which was a little higher but still below 1 mm. The correlation model error and the prediction error demonstrate that their accuracies are comparable to the machine accuracy.

## Discussion

This study demonstrates a real-time DMLC tracking with target position input utilizing data streams of kV/MV imaging systems and external respiratory monitoring system which are

already available from clinical treatment machines. By establishing an internal/external correlation model and updating it with occasional kV/MV imaging, we obtained accurate estimations of real-time target position from external respiratory signals. The benefits of using the proposed hybrid method were the reduction of kV imaging dose and system latency.

Similar to our previous study, we only used an open aperture to prevent occlusion of the fiducial marker by the MLC leaf and also to measure the tracking error directly using MV images. The simple MLC aperture and phantom geometry were used in this study. In practice, however, more complex plans/delivery schemes such as IMRT could have very limited MLC apertures, resulting in occluded marker observations in MV images. This practical consideration poses a challenge for a direct application of the proposed strategy. Use of multiple markers, a marker-visibility-constrained IMRT plan (13), or a monoscopic estimation using a kV imager alone (11) would be potential solutions to address such concern. In addition, the fiducial marker segmentation on clinical x-ray images (especially MV images) is likely to be much more difficult due to poor contrast, interference with patient anatomy. Development of a robust and reliable marker segmentation method is one of the main challenges to clinical realization of this method. However, the marker segmentation failure on MV images due to such complications might not reduce tracking accuracy significantly, unless the internal/external correlation could change rapidly during the treatment time. It is supported by a recent study based on the Synchrony system, which achieved accurate tracking accuracy with the model update every one or several minutes (12).

Potential approaches to reduce the MV beam dose required for correlation model initialization prior to tracking include decreasing the MV beam dose rate and/or increasing the kV imaging frequency to shorten this time interval. Alternatively, pre-treatment kV imaging can be used to build the correlation model for at least two motion components and therefore reduce the tracking error significantly during the model setup period. An even more sophisticated method is to build the correlation model using rotational kV imaging alone (14). Note that this initialization procedure is needed only for the first treatment beam; the established correlation model could be used for the following treatment beams without re-initialization, even though there is a pause between beams.

To test the impact of the beam hold asserted by the leaf speed limit (15) on the tracking accuracy, tracking experiments were repeated with two different collimator angles for one trajectory with large LR motion. As shown in Fig. 6 since the trajectory has large LR motion, (a) collimator at 180° such that the LR motion matched the leaf travel direction. (b) For collimator angle of 270° where LR motion is perpendicular to the leaf travel direction, it shows frequent beam-holds on mid-inhale or exhale where the target moves fast perpendicular to the leaf travel direction. Consequently, even though the delivery time was increased by 10%, the tracking accuracy was similar. However, further reduction of tracking efficiency would be expected as the shape of the treatment field becomes more complex.

Another interesting finding is the impact of external signal noise. Due to the linear relationship in the correlation model between target motion and external signal, external signal noise would directly affect the position estimation accuracy, especially for patients with small external breathing motion relative to the internal tumor motion. In general, the motion range of external signals has a similar magnitude of that of tumor motion, but if the external signal is several times smaller than tumor motion, then external signal noise directly reinforces the target motion estimation error. Fig. 7 shows one example from the tracking experiment that shows the impact of external signal noise on the position estimation. Compared to simulation without external noise, experimental data shows noise of SD=0.1

mm. Since the range of SI target motion is 5 times larger than the external signal, 0.1mm of external noise manifests the error in target position estimation from 0.2 to 0.7 mm. It suggests more accurate respiratory surrogates would be preferable such as a stereo-infrared camera (16) or a stereo-surface imaging system (17).

Finally, it should be mentioned that although we demonstrated the application of the proposed target position estimation method for DMLC tracking, the method can be more easily applicable to gated radiotherapy which is being used in the clinic. Since in gated radiotherapy the external breathing signal alone is often used for target position estimation, the inter- and intra-fractional variation of the relationship between the external signal and the internal tumor position could reduce the accuracy (18). With the proposed method where the external breathing signal can be supplemented by the intermittent x-ray measurement of the internal target position, the accuracy of gated radiotherapy might be significantly improved.

## Conclusion

A novel real-time target position estimation method has been developed and integrated into a DMLC tracking system. Experimental demonstrations of the integrated tracking system have shown that the geometrical error caused by respiratory motion is substantially reduced by the application of respiratory motion tracking. The method uses hardware tools available on linear accelerators and therefore shows promise for clinical implementation. However, to overcome the remaining challenges such as high risk of complications in marker implantation, difficulties in marker segmentation due to the marker occlusion in IMRT fields and the limited image quality, it requires continuing research and development to yield a robust clinical implementation of this approach. We will continue to study the clinical implication of the challenges and continue to develop and validate the clinical implementation of the proposed approach.

## Acknowledgments

This work was supported by NCI Grant R01CA93626. Per Rugaard Poulsen has received financial support from Varian Medical Systems. The authors are grateful for Varian technical support, particularly Herbert Cattell for the dynamic MLC control program, Hassan Mostafavi and Alexander Sloutsky for sharing their own online marker segmentation tool, and Sergey Povzner for the research version of the RPM software with dual-output capability to the OBI and the dynamic MLC tracking systems. We also thank Sonja Dieterich for acquiring and preparing the tumor motion database and Libby Roberts for editing the manuscript.

## References

1. Cho B, Poulsen PR, Sloutsky A, et al. First Demonstration of Combined Kv/Mv Image-Guided Real-Time Dynamic Multileaf-Collimator Target Tracking. International Journal of Radiation Oncology Biology Physics 2009;74:859–867.
2. Wiersma RD, Mao WH, Xing L. Combined kV and MV imaging for real-time tracking of implanted fiducial markers. Medical Physics 2008;35:1191–1198. [PubMed: 18491510]
3. Poulsen PR, Cho B, Ruan D, et al. Dynamic MLC tracking of respiratory target motion based on a single kilovoltage imager during arc radiotherapy. Int J Radiat Oncol Biol Phys. 2009 In press.
4. Schweikard A, Shiomi H, Adler J. Respiration tracking in radiosurgery. Medical Physics 2004;31:2738–2741. [PubMed: 15543778]
5. Malinowski K, Lechleiter K, Hubenschmidt J, et al. Use of the 4D phantom to test real-time targeted radiation therapy device accuracy. Medical Physics 2007;34:2611–2611.
6. Sawant A, Venkat R, Srivastava V, et al. Management of three-dimensional intrafraction motion through real-time DMLC tracking. Medical Physics 2008;35:2050–2061. [PubMed: 18561681]

7. Ruan D, Fessler JA, Balter JM, et al. Inference of hysteretic respiratory tumor motion from external surrogates: a state augmentation approach. Physics in Medicine and Biology 2008;53:2923–2936. [PubMed: 18460744]
8. Keall PJ, Cattell H, Pokhrel D, et al. Geometric accuracy of a real-time target tracking system with dynamic multileaf collimator tracking system. International Journal of Radiation Oncology Biology Physics 2006;65:1579–1584.
9. Srivastava V, Keall P, Sawant A, et al. Accurate prediction of intra-fraction motion using a modified linear adaptive filter. Medical Physics 2007;34:2546–2546.
10. Suh Y, Dieterich S, Cho B, et al. An analysis of thoracic and abdominal tumour motion for stereotactic body radiotherapy patients. Physics in Medicine and Biology 2008;53:3623–3640. [PubMed: 18560046]
11. Cho BC, Suh YL, Dieterich S, et al. A monoscopic method for real-time tumour tracking using combined occasional x-ray imaging and continuous respiratory monitoring. Physics in Medicine and Biology 2008;53:2837–2855. [PubMed: 18460750]
12. Hoogeman M, Prevost JB, Nuyttens J, et al. Clinical Accuracy of the Respiratory Tumor Tracking System of the Cyberknife: Assessment by Analysis of Log Files. International Journal of Radiation Oncology Biology Physics 2009;74:297–303.
13. Ma YZ, Lee L, Keshet O, et al. Four-dimensional inverse treatment planning with inclusion of implanted fiducials in IMRT segmented fields. Medical Physics 2009;36:2215–2221. [PubMed: 19610310]
14. Cho B, Poulsen P, Ruan D, et al. DMLC Tracking with real-time target position estimation combining a single kV Imager and an optical respiratory monitoring system. Int J Radiat Oncol Biol Phys. 2009 Suppl:ASTRO2009 presentation.
15. Wijesooriya K, Bartee C, Siebers JV, et al. Determination of maximum leaf velocity and acceleration of a dynamic multileaf collimator: Implications for 4D radiotherapy. Medical Physics 2005;32:932–941. [PubMed: 15895576]
16. Willoughby TR, Forbes AR, Buchholz D, et al. Evaluation of an infrared camera and X-ray system using implanted fiducials in patients with lung tumors for gated radiation therapy. International Journal of Radiation Oncology Biology Physics 2006;66:568–575.
17. Bert C, Metheany KG, Doppke K, et al. A phantom evaluation of a stereo-vision surface imaging system for radiotherapy patient setup. Medical Physics 2005;32:2753–2762. [PubMed: 16266088]
18. Korreman SS, Juhler-Nottrup T, Boyer AL. Respiratory gated beam delivery cannot facilitate margin reduction, unless combined with respiratory correlated image guidance. Radiotherapy and Oncology 2008;86:61–68. [PubMed: 18039549]

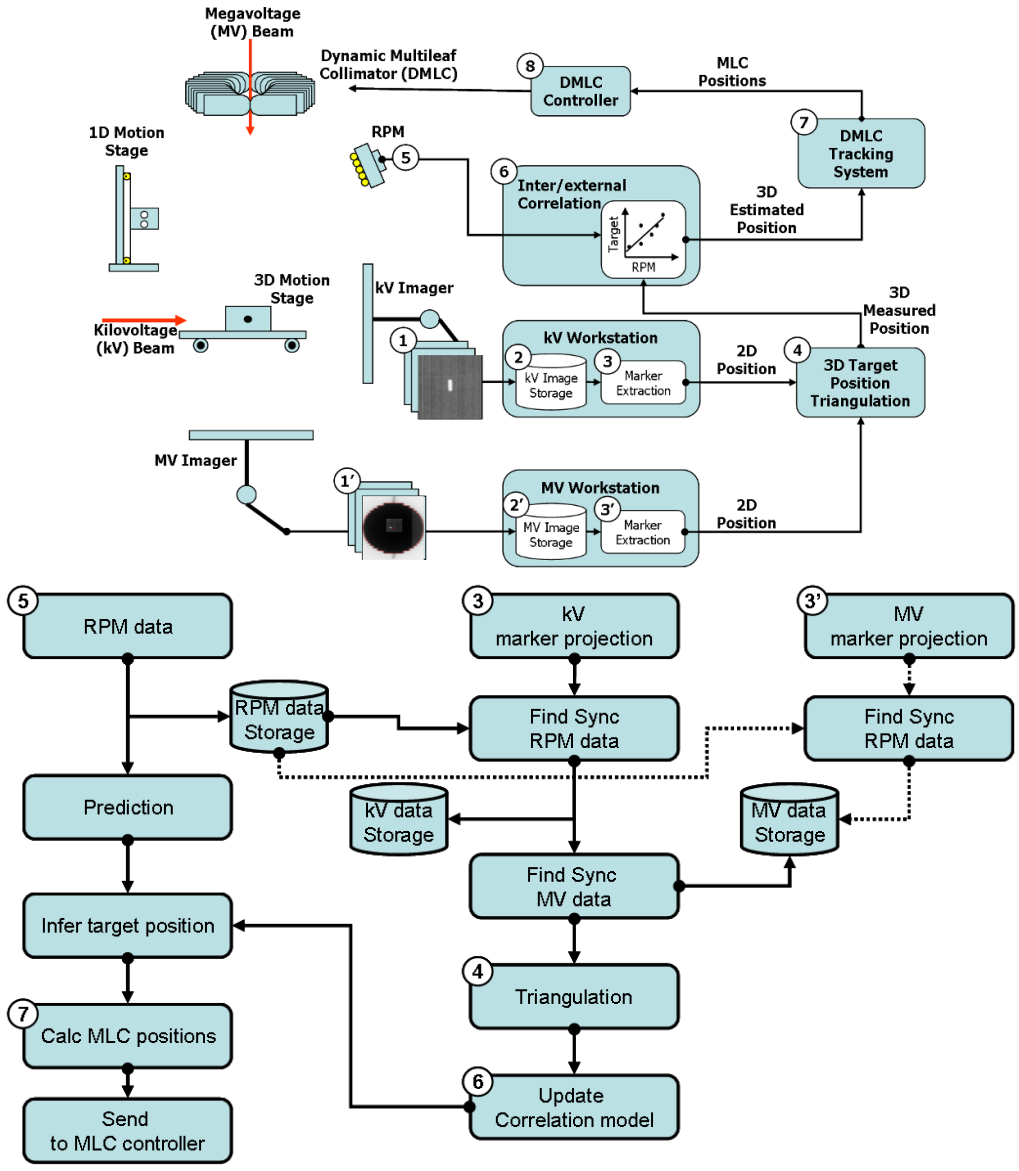


**Fig. 1.**

(a) Overview of an integrated DMLC tracking system and (b) dataflow of kV/MV and RPM inputs in the procedure of real-time target position estimation combining occasional kV/MV imaging and continuous external respiratory monitoring.

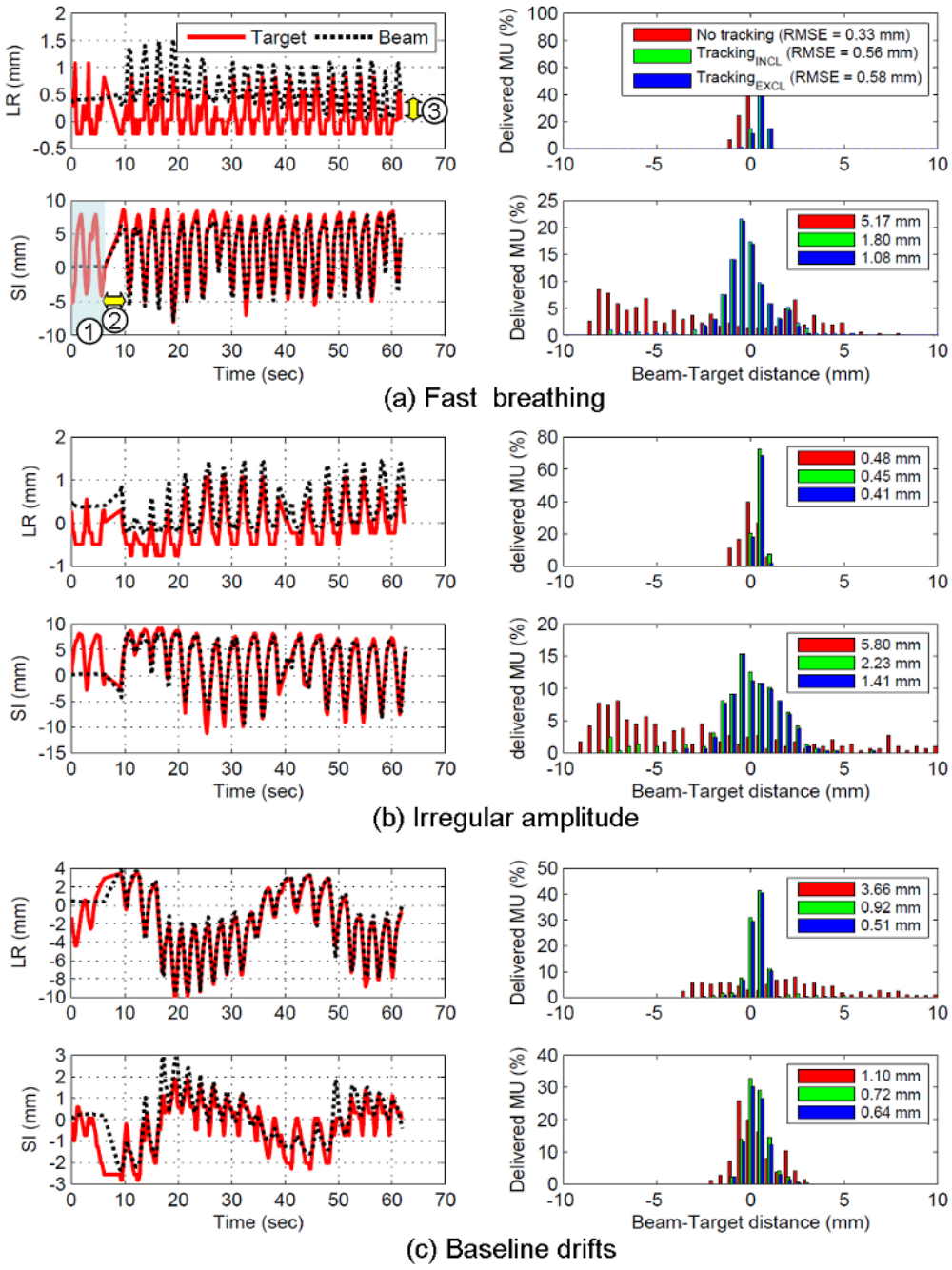


**Fig. 2.**

Beam-target alignment accuracy for 3 tracking examples; (a) fast breathing motion, (b) irregular amplitude, and (c) baseline drifts. The left-right (LR) and superior-inferior (SI) positions are measured from the MV beam isocenter on MV imager, respectively. RMSE means root-mean squared error. Note that ① no tracking period of 6 sec happened after the MV beam started due to the model building period. It was followed by ② a beam hold period of 3 sec due to the >5mm positional difference between the set and actual leaf positions. ③ A systematic shift of 0.4 mm in the LR direction reflects the machine accuracy of the MV beam isocenter. Tracking$_{INCL}$ (or Tracking$_{EXCL}$) means the tracking accuracy including (or excluding) the model building period.

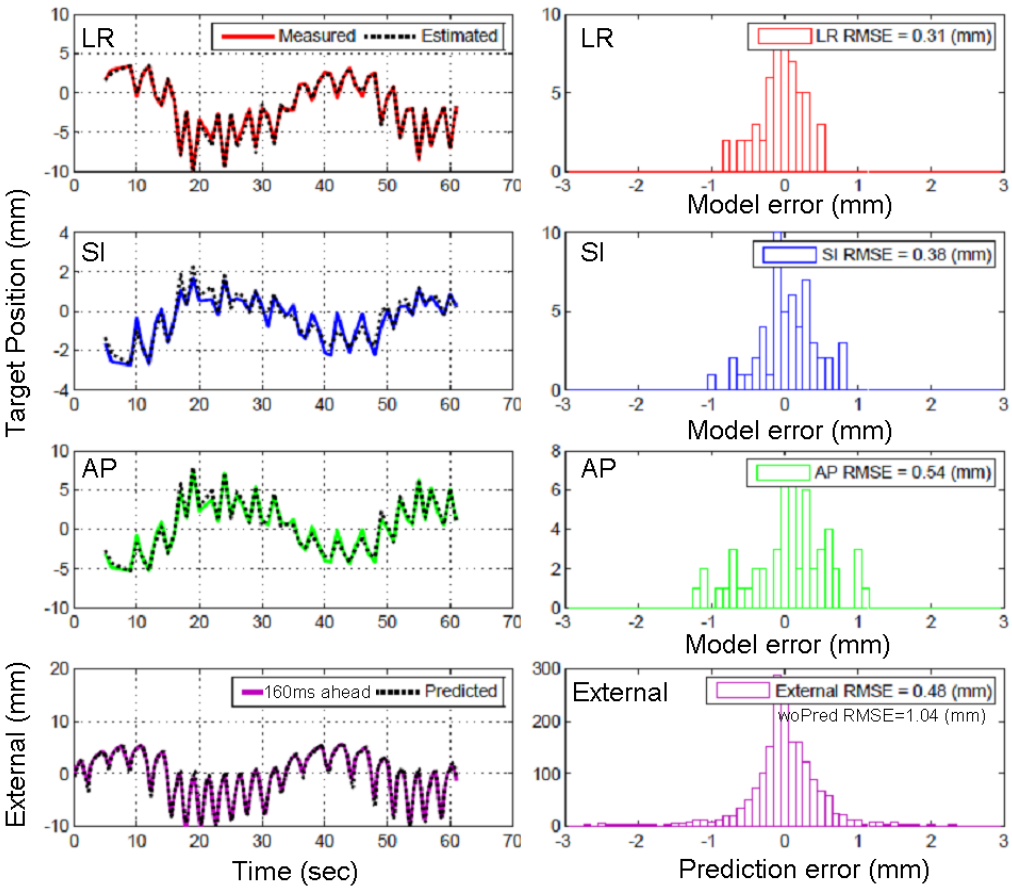


**Fig. 3.**

Example of the correlation model and prediction error for the case (c) in Fig. 2. The upper 3 rows represent the correlation model error in each direction that measures the difference between the measured and estimated target positions, and the bottom row corresponds to the prediction error that measures the difference between the predicted and actual input of 160ms ahead.

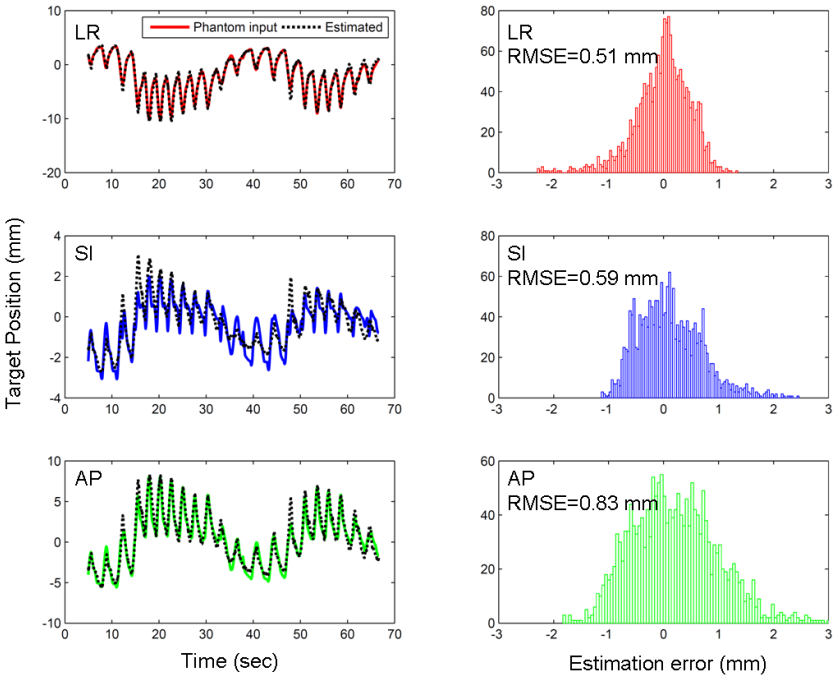


**Fig. 4.**

Example of the target position estimation error for the same trajectory (c) in Fig. 2.

*footnote: the scales of the y-axis in each direction are different to illustrate the result better.

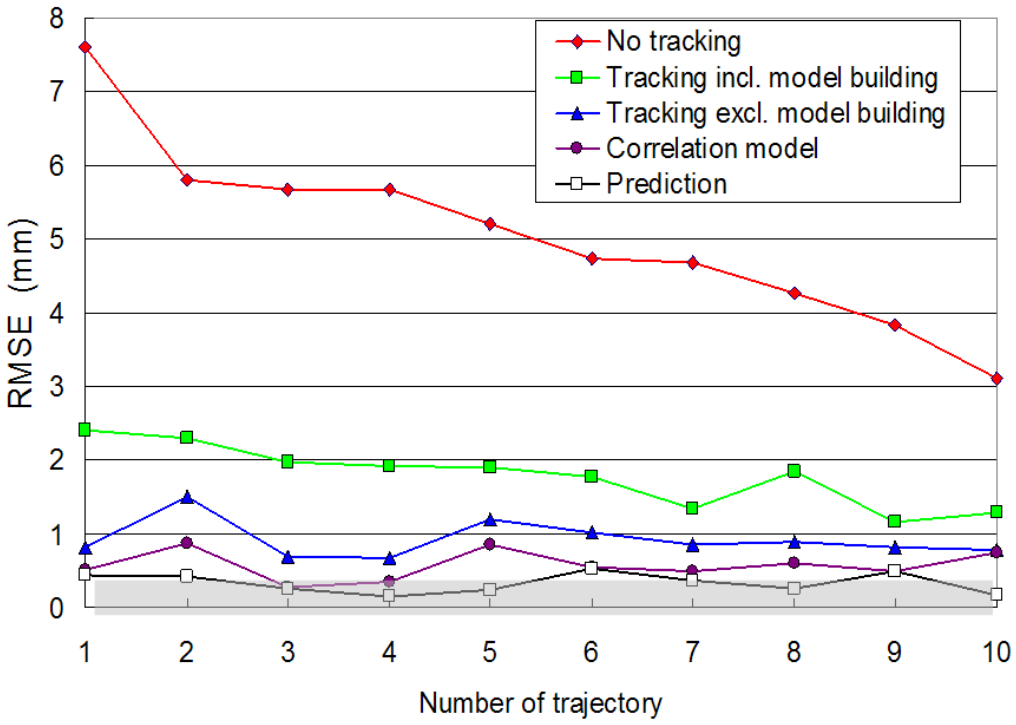


**Fig. 5.**

Beam-target alignment error with and without tracking for 10 experimental trajectories. The gray region represents the 0.5-mm machine accuracy of the MV beam isocenter specified by the manufacturer. The correlation model error and the prediction error demonstrate that their accuracies are comparable to the machine accuracy.

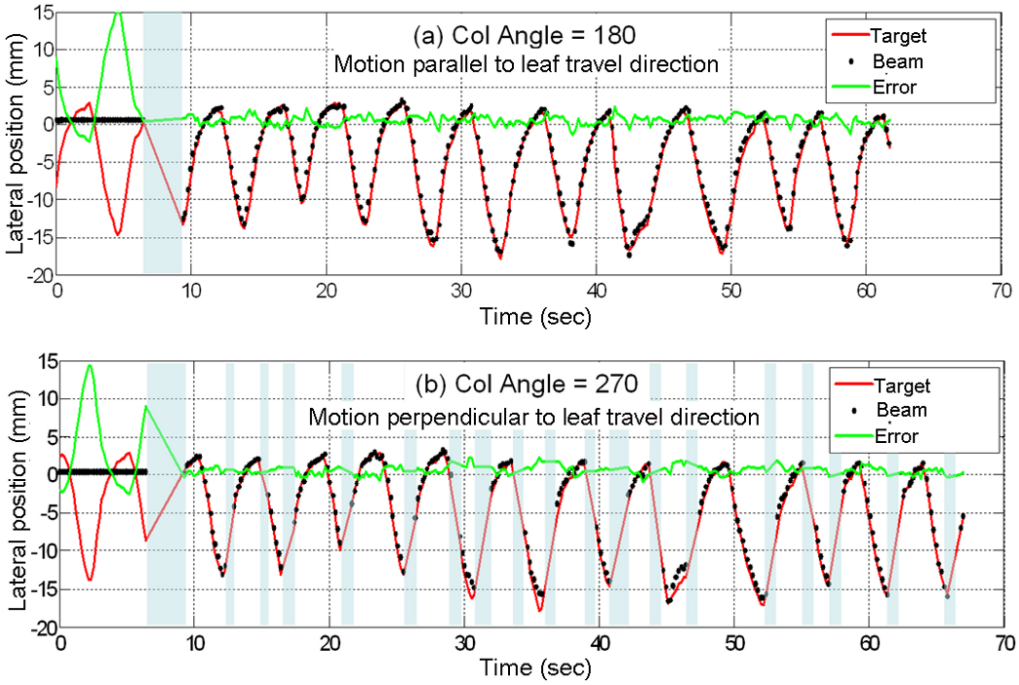


**Fig. 6.**

Comparison of target vs. MLC trajectory of a large lateral motion tumor trace for two different collimator angles. (a) Collimator at 180° such that the lateral motion matched the leaf travel direction. (b) Collimator angle of 270° where lateral motion is perpendicular to the leaf travel direction. The gray-colored time periods represent beam-hold intervals caused by the leaf speed limitation.

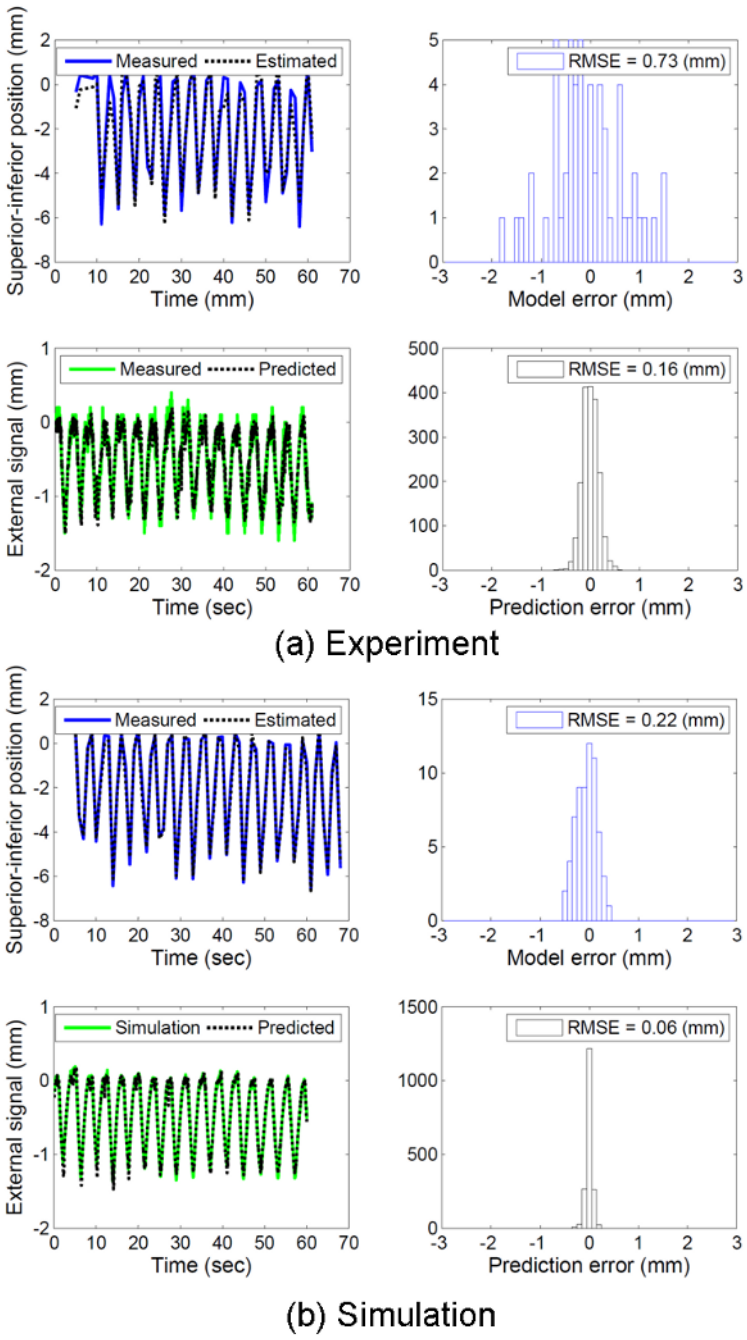


**Fig. 7.**
Experimental results with external signal noise vs. simulation results without external signal noise.